MARCH 1974

. ATL TR 195

METHODOLOGY FOR THREE DIMENSIONAL
NOZZLE DESIGN

By
A. Ferri, S. Dash and
P. Del Guidice

1. Nozzles -- Design

PREPARED FOR

NASA LANGLEY RESEARCH CENTER
HAMPTON, VIRGINIA 23665

UNDER

CONTRACT NO.: NAS1-12104

BY

ADVANCED TECHNOLOGY LABORATORIES, INC.
Merrick and Stewart Avenues
Westbury, New York 11590

INDEX

LIST OF FIGURES

SECTION I

INTRODUCTION

The selection of the nozzle design for a hypersonic scramjet should be done based on a compromise of external and internal flow requirements, related to drag, lift, and pitching moments of the vehicle, and thrust of the engine. In addition, structural and weight considerations should be included therefore, a complex design study is required based on engineering judgement that cannot be obtained solely from complex numerical programs. In the preliminary design stage, a logical sequence appears to be first obtaining a satisfactory aerodynamic design criteria, and then refining this by introducing weight and structural considerations. The present work is directed toward developing criteria for selection and methods of analysis directed toward definition of a satisfactory aerodynamic design.

The methodology employs three steps differing in levels of sophistication.

> STEP 1 - In this initial step, the effects of many parameters involved in performance are evaluated on the basis of a simplified wave analysis in order to determine their relative importance and their appropriate values.

This first phase is devoted toward selecting the location, size and expansion ratio of the engine streamtube and the ratio between the expansion in the transverse direction to the expansion in the direction normal to the engine.

Figure (1) is a schematic of the important vehicle-engine parameters; where the lift is given by the suction force on the upper surface L_2, by the spillage pressure L_1, by the engine cowling pressure L_4, (which is a function of σ_2) and by the expansion of the engine L_3. The engine divergency in plan view σ_1 induces a lift L_5, and the divergency of the jet σ_3 contributes to L_3.
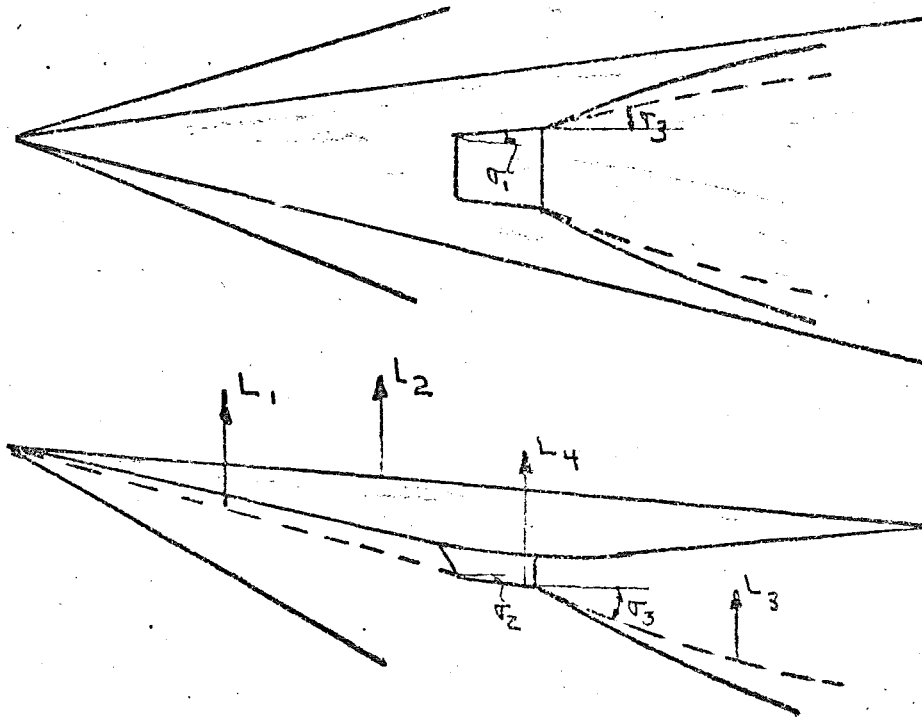
FIGURE 1.

STEP 2 - This step involves the use of a "source flow" charac-
teristic analysis; approximate values of lift, thrust
drag and pitching moments are obtained using the range
of parametric values determined in Step 1. Additionally,
the influence of the nozzle on the external flow will be
evaluated employing two dimensional and conical flow ap-
proximations.

STEP 3 - As a result of Steps (1) and (2) the values of the main
parameters are approximately known and preliminary per-
formance levels have been obtained. Then, the most
promising configurations can be analyzed in detail.

A brief description of the simplified wave analysis of Step 1 is presented
in Section II of this report. A numerical procedure incorporating the ideas
outlined in this section has been developed and is described in detail in
Reference (1).

The "source flow" approach is briefly discussed in Section III. A complete
description of this technique and its application to the analysis of scram-
jet exhaust flow fields is contained in Reference (2), while a description
of the numerical program and user manual is given in Reference (3).

A description of the vehicle-engine interference is contained in Section IV.
The analysis provides for determination of a preliminary exhaust plume shape
based on quasi-two dimensional considerations as well as an assessment of
the cowling lift and drag based on quasi-conical flow solutions.

Steps (1) and (2) yield a preliminary estimate of the range of nozzle para-
meters to be considered. After completion of this preliminary design work
a full three dimensional calculation can be made using analysis and the
program described in References (4), (5) and (6). This will permit further
design refinements and the exact computation of thrust, drift and pitching
moment for the vehicle. Thus, lengthly three dimensional calculations are
avoided until simpler parametric or quasi two dimensional calculations have
defined the basic nozzle configuration. The present approach allows the
nozzle designer to simply investigate and assess the effects of various para-
meters prior to employing three dimensional calculations.

SECTION II

PARAMETRIC APPROACH EMPLOYING SIMPLE WAVE TECHNIQUES

The type of nozzle considered is depicted in Figure (2) and is seen to be a combination of several nozzles merging into a single nozzle. The individual nozzles, before merging, expand the flow in two perpendicular planes as depicted in Figure (3). In this figure, the lateral expansion is depicted as occurring within two parallel walls. However, more general configurations can be considered which require a greater amount of lateral expansion and, hence, require diverging walls in the region of the individual nozzles as depicted in Figure (4).

In the preliminary analysis of Step 1, it is assumed that the jets, after merging, are bounded by sidewalls which extend downstream of the merged station. Then, each nozzle can be analyzed by considering two regions. The first region extends from the burner exit to the station at which the individual jets merge (Station A-A of Figure 3), while the second region is that downstream of the merged station. Note that the side expansion of the nozzles produces external compression. This lateral deviation is beneficial since for a given value of total expansion it decreases the deflection angle of the exiting jet flow in the vicinity of the cowl. At the same time, the corresponding external compression does not yield too much of a drag penalty since the compression waves generated are reflected on the rear part of the wing resulting in lift and a decrease in drag due to the wing.

A main consideration of this analysis will be to select the range of important parameters to be considered. The initial flow (at the burner exit) is assumed known and is represented as an average uniform flow, obtained by properly averaging the actual flow at the burner exit station. The assessment of changes introduced by flow nonuniformities at the entrance station is performed in Step 2 of the analysis. The parametric analysis is performed in conjunction with isentropic expansions from uniform initial conditions.
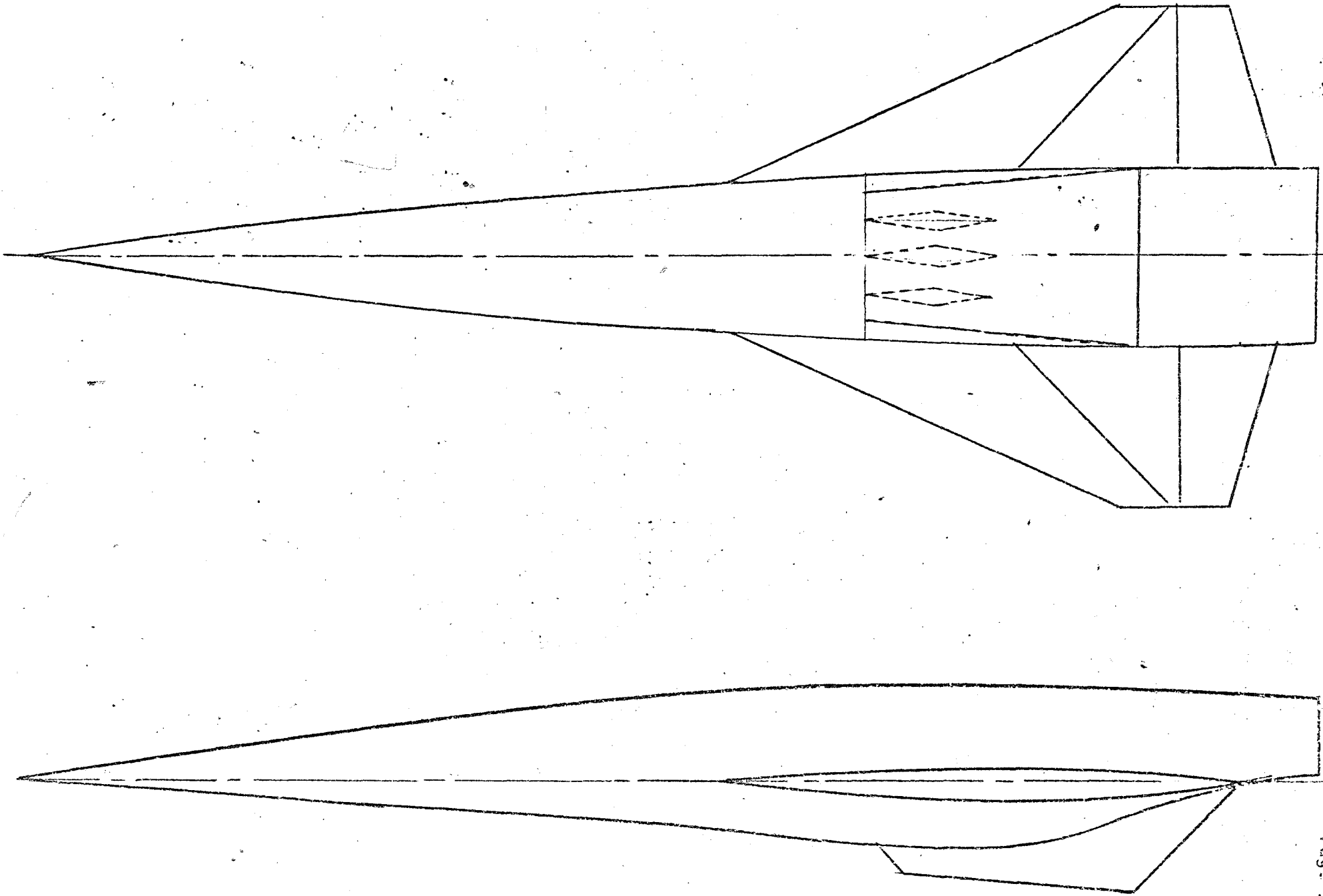
FIGURE 2. TYPICAL VEHICLE - ENGINE INSTALLATION
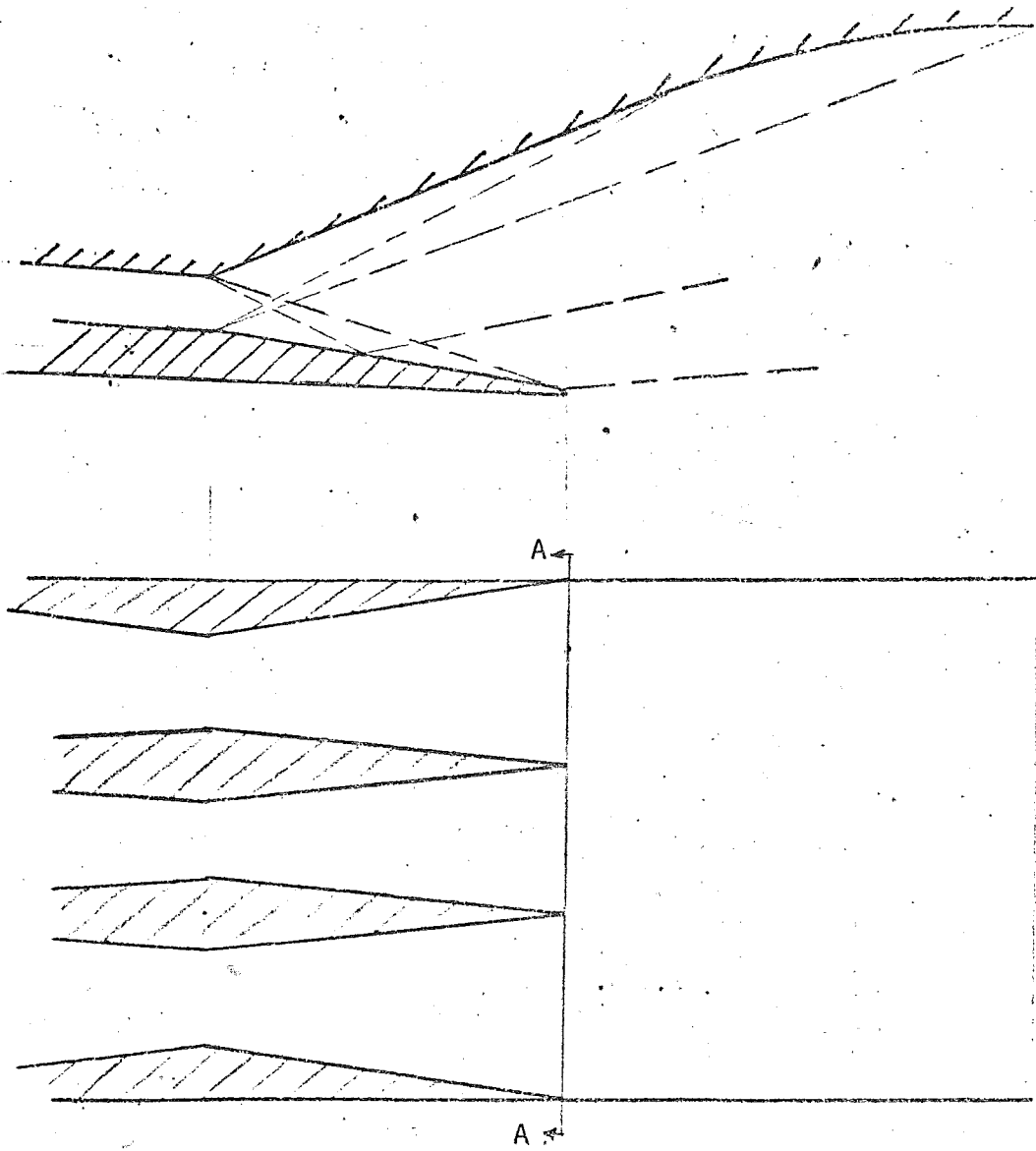
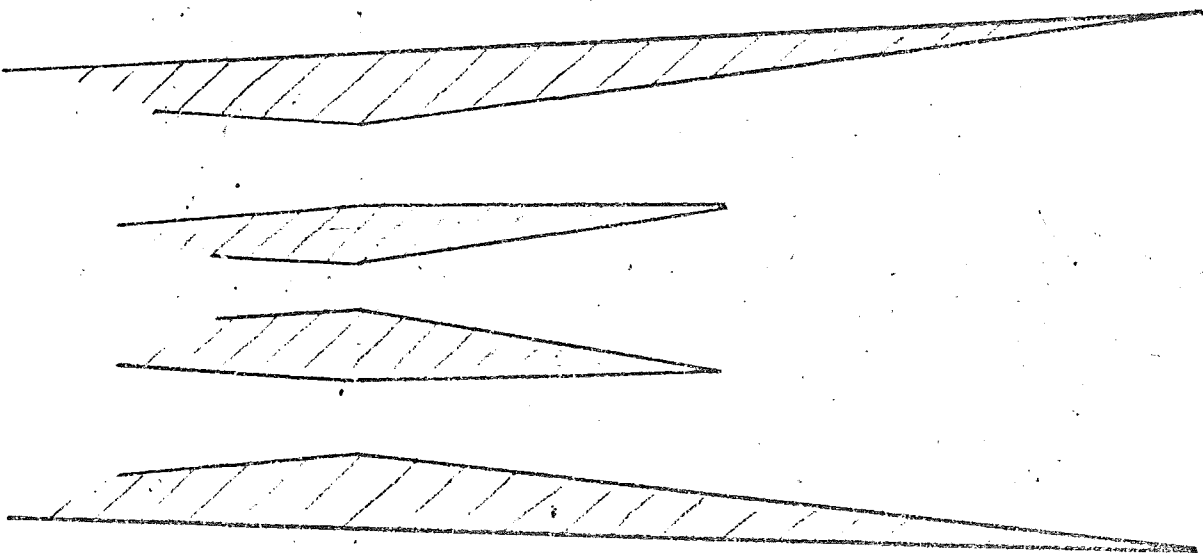FIGURE 3.   INTERNAL NOZZLE SHAPES

FIGURE 4.   INTERNAL NOZZLE SHAPES WITH ADDITIONAL
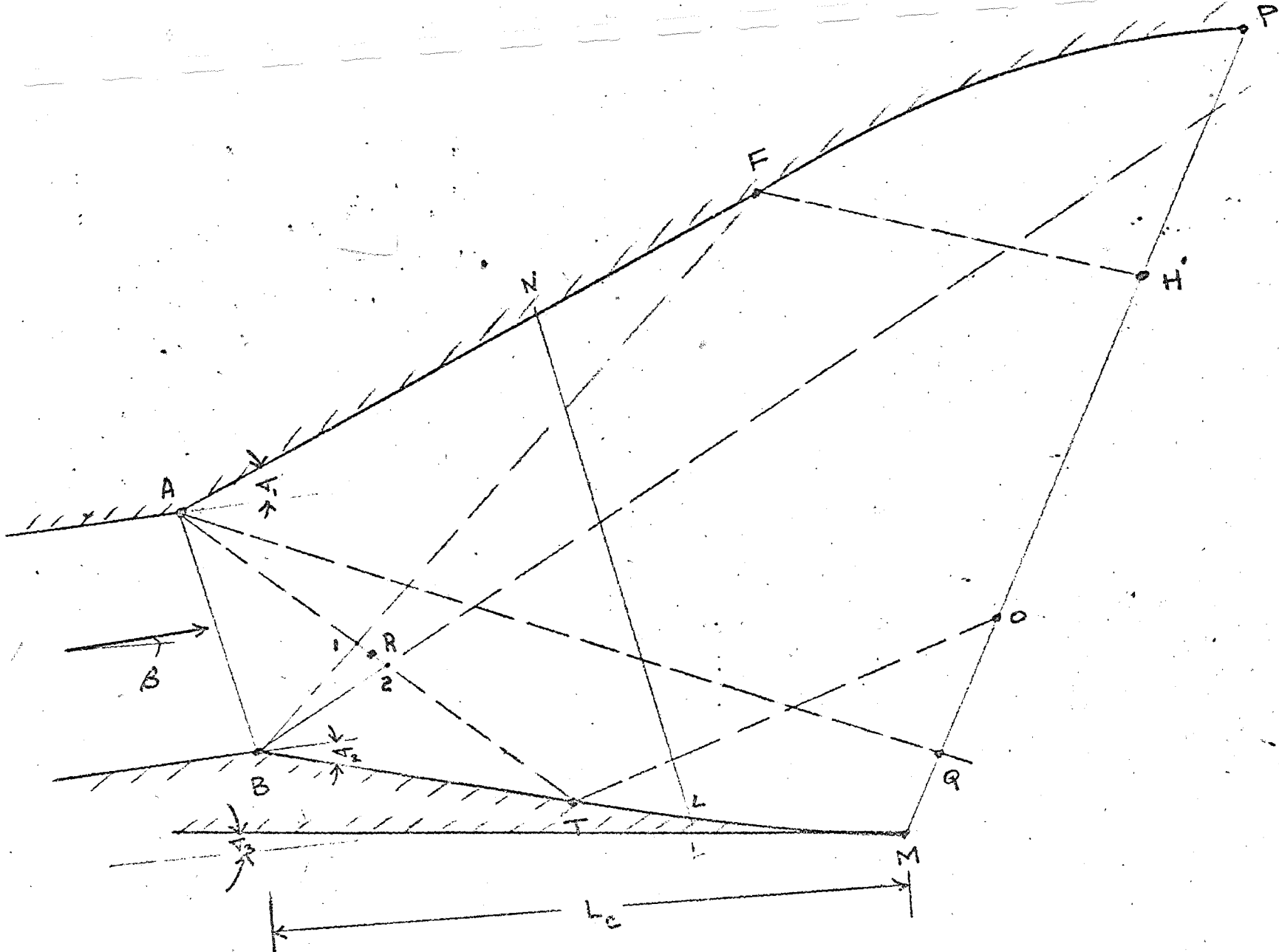   LATERAL EXPANSION

FIGURE 5. WAVE DIAGRAM

Initially assume that the sidewalls are straight and extend to the end of
the nozzle, such that the flow is entirely contained within the sidewall.
Additionally, assume that the internal vertical walls terminate along a
line LN, parallel to the initial line AB which represents the burner exit
station as depicted in Figure (5).

It should be noted that the flow properties can be determined in separate
steps due to the segmenting afforded by the waves of the flow field. At
the nozzle exit, several distinct regions of the flow can be defined.

The segment MQ is dependent on the vertical expansions σ_1 and σ_2 as well as
on the lateral expansion. If the lower cowl length (L) is sufficiently long,
some of the expansion waves generated at A will be reflected and the region
MO is additionally affected by this reflected wave (where the position of 0
may be above or below that of Q).

The first reflected wave from the upper wall reaches the exit station at
point H, hence the flow between Q and H (or 0 and H) undergoes the dual ex-
pansion σ_1 and σ_2 but receives no reflected waves. The waves generated or
reflected at the upper walls cross the exit line between H and P and have an
important effect on the vehicle pitching moments. Note that these waves can
be either expansions or compressions. The value of the turning at the cowl
(σ_2) is a function of σ_3 and the cowl length L as well as the amount of re-
compression introduced between B and M.

Consider the optimum nozzle that can be obtained for a fixed area - i.e.,
the lengths, shapes and turning angles are arbitrary. Optimum conditions
require that the exit flow be parallel to the free stream and the exit pres-
sure be constant for a uniform initial flow field. Such a nozzle is one
where the region OH extends across the entire exit flow station, thus, the
cowl and vehicle lengths and recompressions are such as to cancel the expan-
sions emanating from A and B. The turning angles σ_1 and σ_2 must be selected
such that $\sigma_1 - \sigma_2 = \beta$ where β is the initial flow inclination with respect

to the external flow field. Such an "ideal" nozzle will generally result in excessive cowl and possibly vehicle lengths.

For the real nozzles considered, the expansions produced at A and B will not be fully captured thus producing a nonuniform exit flow. In the uniform region OH, the expansion results from a turning through $\sigma_1 + \sigma_2$ plus the lateral expansion, and the flow deflection angle equals $\beta + \sigma_1 - \sigma_2$. In regions HP and OM, the resultant expansion is dependent on the percentage of the waves from A and B that are reflected and the recompression introduced in these regions. The resultant reflected waves can be either expansion waves or compression waves. Note that if the reflected waves are compression waves, they tend to decrease the exiting velocity and the local Mach numbers, yielding a maximum Mach number in the region OH.

For those nozzle flow fields where a uniform region such as OH occurs at the exit station, the flow field between M and H is independent of the vehicle geometry between A and P. A value of σ_1 is assumed and for this value, several values of σ_2 are considered. The first down-running characteristic from A (ART) determines the minimum cowl length required to obtain reflection at the lower cowling. This line is first obtained two dimensionally ($[\theta-\mu]_{AR} = (\theta-\mu)_A$; $[\theta-\mu]_{R_2T} = \theta_3 - \sigma_2 - \mu_T$ where μ_T represents an expansion by a turning angle of $\sigma_2 - \beta$. After obtaining the two dimensional position of point T, a correction is introduced in terms of the area ratio due to lateral expansion between B and T. This correction is introduced as follows: the Mach number obtained at T from two dimensional considerations defines an area ratio in expansion from the burner Mach number to M_T. This value is multiplied by the value of the lateral expansion ratio ($z_T . z_i$) and this new expansion ratio yields a new (larger) Mach number M_T' and the line RT is redrawn employing the value of μ_T' based on the modified Mach number.

Employing this procedure, several other characteristic lines corresponding to different values of turning at point A ranging from 0 turning to σ_1 may be

determined and thus the lines AL, AM and AQ may be generated, with similar procedures used to obtain the corresponding reflected waves.

From the wave diagram constructed, the value of thrust for the mass contained between M and H may be determined for several values of σ_1, σ_2, L and recompression between T and M. The thrust obtained depends only on these parameters and does not depend on the shape of the vehicle undersurface between A and P. The calculation may be first performed for a straight lower cowling (BM straight). After, some wave cancellation can be easily introduced for each value of L between T and M and the optimum value obtained by trading off a reduction in expansion for a decrease in flow angle at the exit station.

For each value of σ_2 chosen, a curve is obtained yielding the variation of thrust (Th) as a function of σ_1 for a given value of L and, hence, a curve of σ_1 vs. L with thrust as a parameter can be generated.

In order to optimize the calculation for the values of σ_1, L and σ_2 selected the following possibilities are investigated; zero reflection and cancellation, total reflection and half reflection. For each case, the position of M is determined and the external drag is obtained. Then, the thrust of the mass crossing MH minus the drag is plotted in terms of percent reflection and the optimum value obtained for each set of L and σ. The loss in thrust in percent as compared to the optimum is used as a parameter for comparison.

Now, the flow between H and P may be analyzed. For this analysis, the values of σ_1 selected for the analysis of the lower region are considered for a given value of σ_2, hence the variable is the curvature of FP. For each variation of the height M, an equivalent variation of the height of P is chosen which then defines the curvature of FP (if a parabolic recompression is selected) and the thrust of HP is obtained.

After performing this analysis for several values of σ_2, the range of parameters which require more accurate analysis are defined and approximate values of forces are also obtained. This approach is quite simple since changes in

σ_1 and σ_2 require only the addition of several waves. The same is true for changes in reflections.

SECTION III
SOURCE FLOW CHARACTERISTIC APPROACH

Step (1) of the design process has defined the overall nozzle expansion ratio, the transverse to longitudinal expansion ratio and the approximate cowl length. This next phase serves to refine this data and fill in the details of the nozzle shape. This approach will be based on quasi two dimensional considerations.

In the preliminary design of the vehicle undersurface and cowl the quasi two dimensional approach must consider, at least to a first approximation, the lateral extent of the nozzle. Consider the following: the basic NASA scramjet/ramjet design philosophy assumes multiple injector burner configurations. The burner flow can be separated into regions with combustion occurring at different longitudinal stations; expansion of the flow begins in the combustor and continues into the nozzle. The resulting wave pattern directly influences nozzle performance.

Figure (6) is a schematic of a multiple burner design which results in a lateral distribution which may be roughly approximated by a line source type flow, which more closely approximates the physical case than the usual two dimensional conditions assumed, which correspond to single injector designs. The burner flow to a first approximation (neglecting shock waves) can be represented by an average velocity, but gradually changing direction, as in a source type of flow.

In the present approach, the lateral extent of the nozzle will be treated as a cylindrical source term in the first pass design of the vehicle undersurface and cowl. This produces a three dimensional effect, but does not account for side wall curvature and shock losses. However, during the course of the calculation it will be possible to specify, at a given axial station, a change in the origin of the source flow. This corresponds to a change in the lateral wall angle σ as shown in Figure (7).
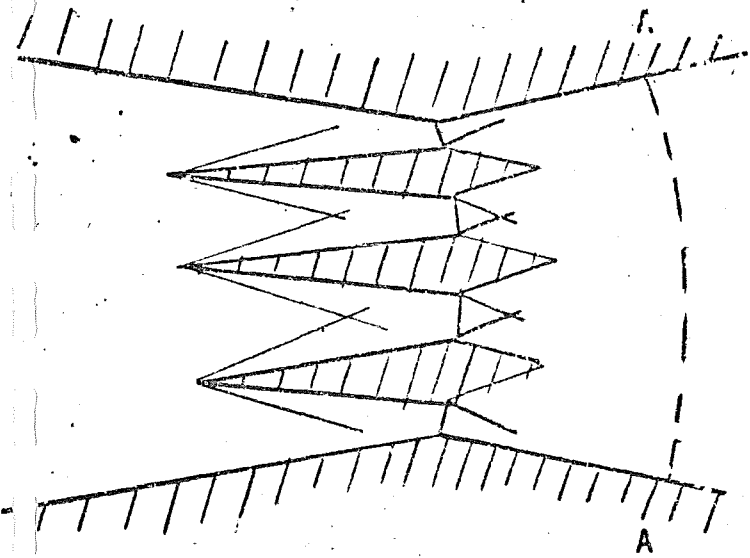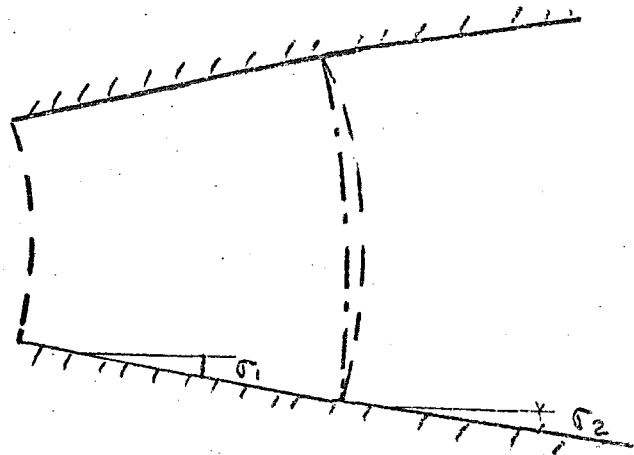
FIGURE 6

FIGURE 7

The same flow technique is employed in conjunction with a two dimensional second-order characteristic procedure capable of analyzing the aerodynamic performance of typical nozzle configurations selected from simplified analysis. Such a configuration is depicted in Figure (8).
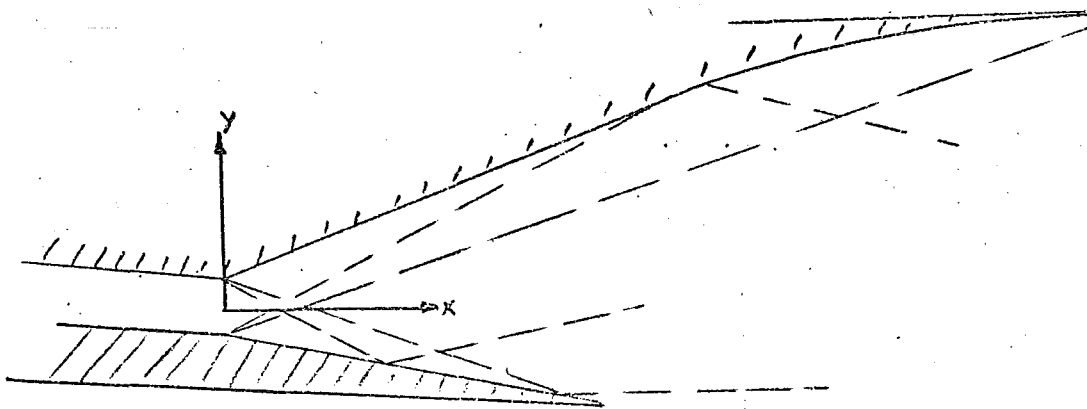
FIGURE 8. TYPICAL SCRAMJET NOZZLE

However, the calculation procedure is not limited to these configurations but can be readily adapted to calculate other two dimensional configurations. This generality results from the use of three coordinates systems, axisymmetric, axially expanding (source type flow) and Cartesian (plane two dimensional), as described in detail in references (2) and (3). Automatic provisions for switching from axially expanding to Cartesian coordinates at a specified axial station and multiple source origins are provided for. These features allow the lateral nozzle area variation to be accounted for in a quasi-two dimensional manner. A higher order calculation would involve a fully three dimensional calculation which would locate the lateral waves.

The working fluid is assumed to be a hydrogen-air mixture in frozen or chemical equilibrium.

The following boundary conditions are provided for in the calculation.

       (1)   Wall boundaries

       (2)   Shock boundaries

       (3)   Contact surface

       (4)   Underexpansion interaction

       (5)   Overexpansion interaction

       (6)   Prandtl-Meyer

A running integration of pressure on the nozzle surfaces is performed which yields thrust, lift and pitching moment in vehicle coordinates.

SECTION IV

ANALYSIS OF ENGINE-VEHICLE INTERFERENCE EFFECTS

For our purposes engine-vehicle interference effects will be classified into two categories;

      a)   Forces due to the presence of the engine plume

      b)   External cowl and/or fence forces

The establishment of suitable engineering criteria for the computation of these forces, within the context of a parametric nozzle analysis, are derived from linearized supersonic flow. Conical flow relations are employed in corner regions of the external flow, and use is made of the concept of preservation of lift as an interference effect [7]. The latter results in a very useful integral relation which is applicable to nonlinear flow fields. The conical nature of the external cowl flow field, yields a closed form solution for the corner pressure distribution. In addition, a simple correlation for the interference pressure in an internal compression corner has been developed.

      A.   Plume Interference Analysis Preservation of Lift as an Interference Effect - Consider a wing, as discussed in reference (7), with supersonic edges whose trailing edge is perpendicular to the flow direction as in Figure (9a). The lift coefficient due to the deflected element has the two dimensional value $4\alpha_o$ $(M_\infty = \sqrt{2})$, when based on the area of the deflected element. This concept may be viewed as an interference effect, since the undeflected part of the wing, while generating no lift, helps preserve the lift of the deflected part. Now consider the wing in Figure (9b). If the undeflected area to the right of CF were removed, the edge CF would be subsonic and (for $\alpha_o > 0$) the lower surface affects the upper surface via an upwash field. Thus, the lift in the triangle CEF would only have half of its two dimensional value. If the flat plate at zero angle of attack is reinserted it gets a positive apparent angle of attack due to the upwash field, and will carry positive lift. Thus the interference is favorable. Furthermore, the interference is mutual; the lift due to the apparent angle of attack on the right half will induce additional lift on the left half, etc.

The final result of this mutual interference is that all the lift is preserved. In using the word "all", the two dimensional value is the standard of comparison. However, only part of the lift is carried by the deflected part. The remainder is carried by the undeflected part.
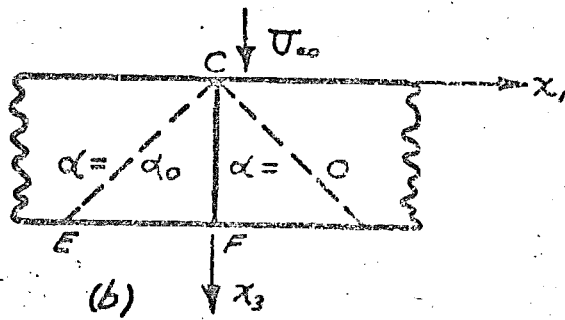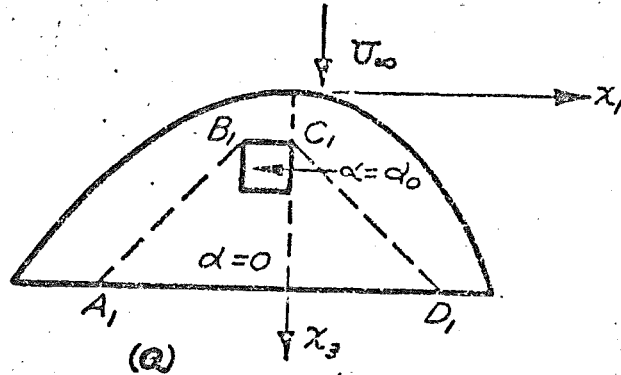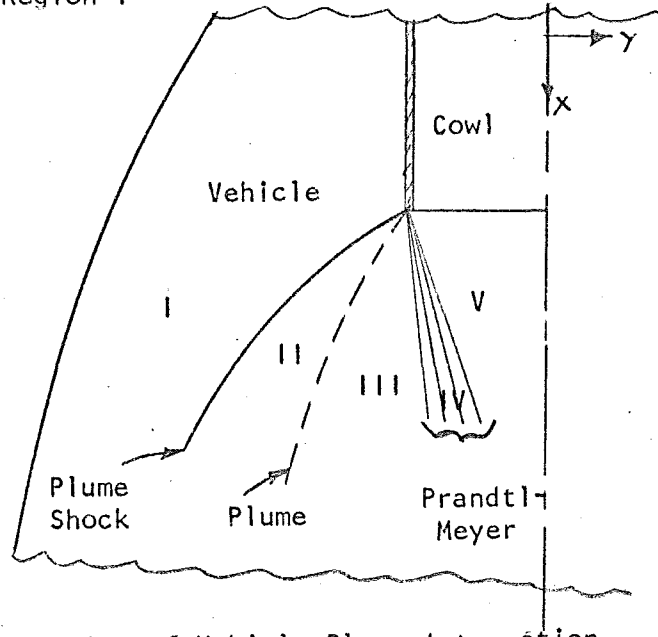

FIGURE 9

Consider the underexpanded nozzle exhaust flow field shown in plan view in Figure (10a). Region I

Plan View of Vehicle-Plume Interaction

FIGURE 10a

is the local undisturbed external flow, Region II is the disturbed external flow, Regions III, and IV are the disturbed exhaust flow and Region V is the undisturbed exhaust flow. The normal force is defined as the integral

$$\sum_i \int_{A_i} P_i dA_n = F_{n_1}$$

Now assume that the nozzle exhaust were separated from the undisturbed vehicle flow by a plate ab as in Figure (10b). The normal force is defined as the integral

$$\sum_{I,V} \int_{A_i} P_i dA_n = F_{n_2}$$
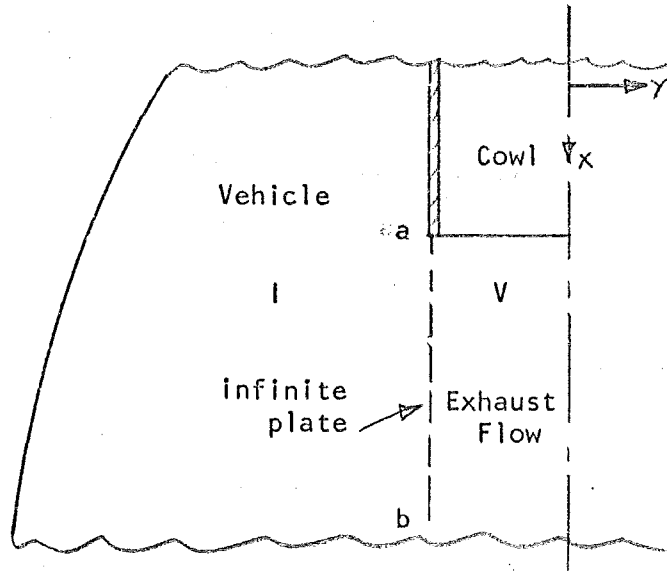
Plan View of Vehicle

FIGURE 10b

From the theorem of Preservation of Lift $F_{n1} = F_{n2}$. This may be illustrated by the following simple example. Define the flow in Region I, and V as

$$P_V = 10 \; P_I \qquad\qquad P_I = 1$$

$$M_V = 3 \qquad\qquad M_I = 8$$

$$\gamma_V = 1.25 \qquad\qquad \gamma_I = 1.4$$

$$A_V = A_I \qquad\qquad A_I = 1$$

Then $F_{n2} = 11 \; P_I$. Using the above conditions and computing the integral of the pressures in Regions I, II, III, IV, and V, yields a value of $F_{n1} = 10.9 \; P_I$. Similar results were obtained by performing the indicated computation for other arbitrary flow conditions.

Thus the concept of preservation of lift yields the following general result: "The integrated force for the complete flow field can be determined from the equivalent two dimensional pressure distribution; i.e., replacing the plume by plate ab and computing the equivalent two dimensional flow yields the same integrated force".

However, since the plume is three dimensional an additional concept relating the integral of the disturbance pressure on the vehicle to the integral of the disturbance produced along the vertical plate (see figure 10c) is required in order to apply the preservation of lift theorem. That is the concept must be generalized to disturbances originating on the plate above the vehicle undersurface.
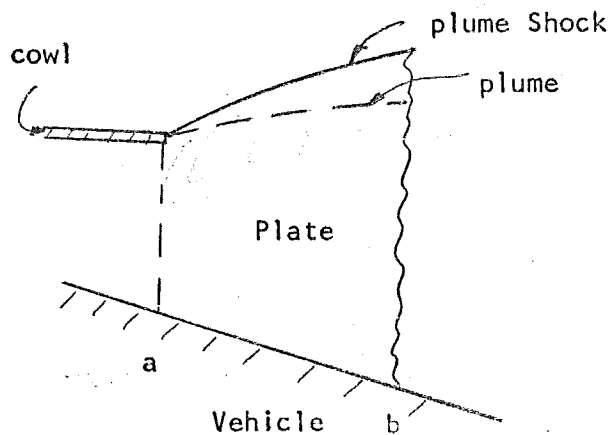
Side View of Plate

FIGURE 10c

The extension of these concepts to three dimensional flow fields is discussed below within the framework of linearized flow.

Integrals of source induced flow fields: Consider a semi-infinite horizontal elemental surface QR having width $\delta\tau$ aligned in the streamwise direction as in Figure (11). The strip is at a distance ζ from the x-y plane and has a source intensity $f(\xi)$ associated with a disturbance pressure ΔP. The trace of the Mach cone from Q on the x,y plane is denoted by ACB. The intersection of the Mach plane from point p with the x-y plane is the line AB. From Reference (8) the following integrals are shown to be valid.

$$\int_A^B \delta u \, dy = U_t(P)\delta\omega = -(\pi f(P)/\beta)\delta\omega$$

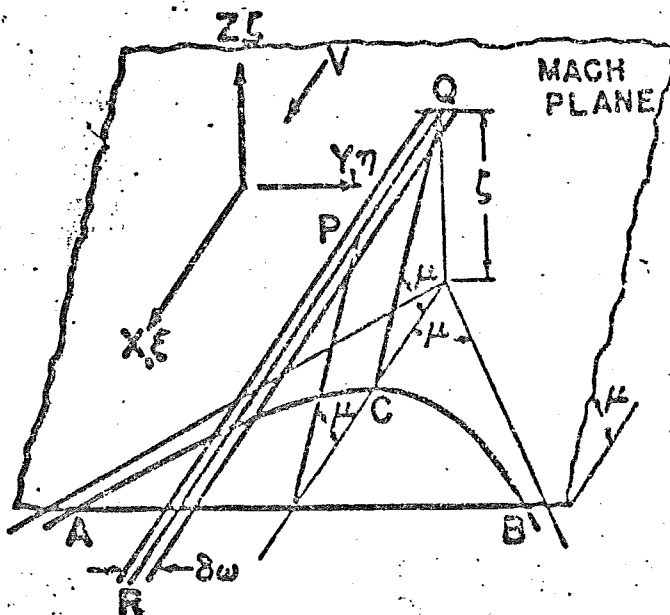$$\int_A^B \delta w \, dy = W_t(P)\delta\omega = -f(P)\delta\omega$$

FIGURE 11

The equations thus yield useful insight into the lateral spreading of disturbances in three dimensional flows. If the distance $\zeta \neq 0$ then the above results apply even if the surface element is rotated about its streamwise axis. If in the limit $f(\xi) \, \delta\omega \to F(\xi)$ then from the above and Figure (12) we obtain

$$\int_A^B \delta u \, dA = - (\pi f/_\beta) \, \delta\xi\delta\omega$$

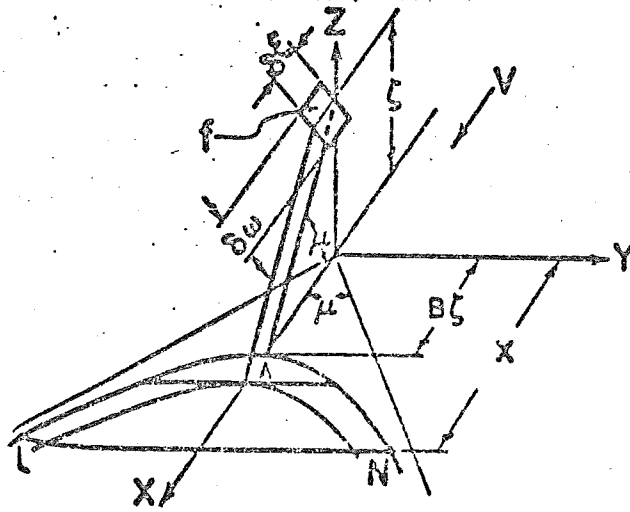$$\int_A^B \delta W \, dA = + (\pi f) \, \delta\xi\delta\omega$$

FIG. 12 Integral relations.

Replacing the source distribution by the disturbance pressure associated with the presence of plate ab leads to the following conclusion. The integral of the disturbance pressure on the vehicle is equivalent to the two dimensional values; i.e., since the disturbances on either side of the plate are equal and of opposite signs the resultant interference effect is equivalent to a quasi two dimensional computation in the presence of plate ab. This is the three dimensional counterpart of the simple two dimensional result illustrated previously.

For linearized flow the above result is exact since disturbances on either side of the plate propagate at the same free stream Mach number. As the Mach numbers can differ substantially on either side of the plate (see Figure 13) corrections must be introduc ed for these differences. This is readily accomplished since the shape of plate ab is known and the Mach lines are given by the characteristics solution.
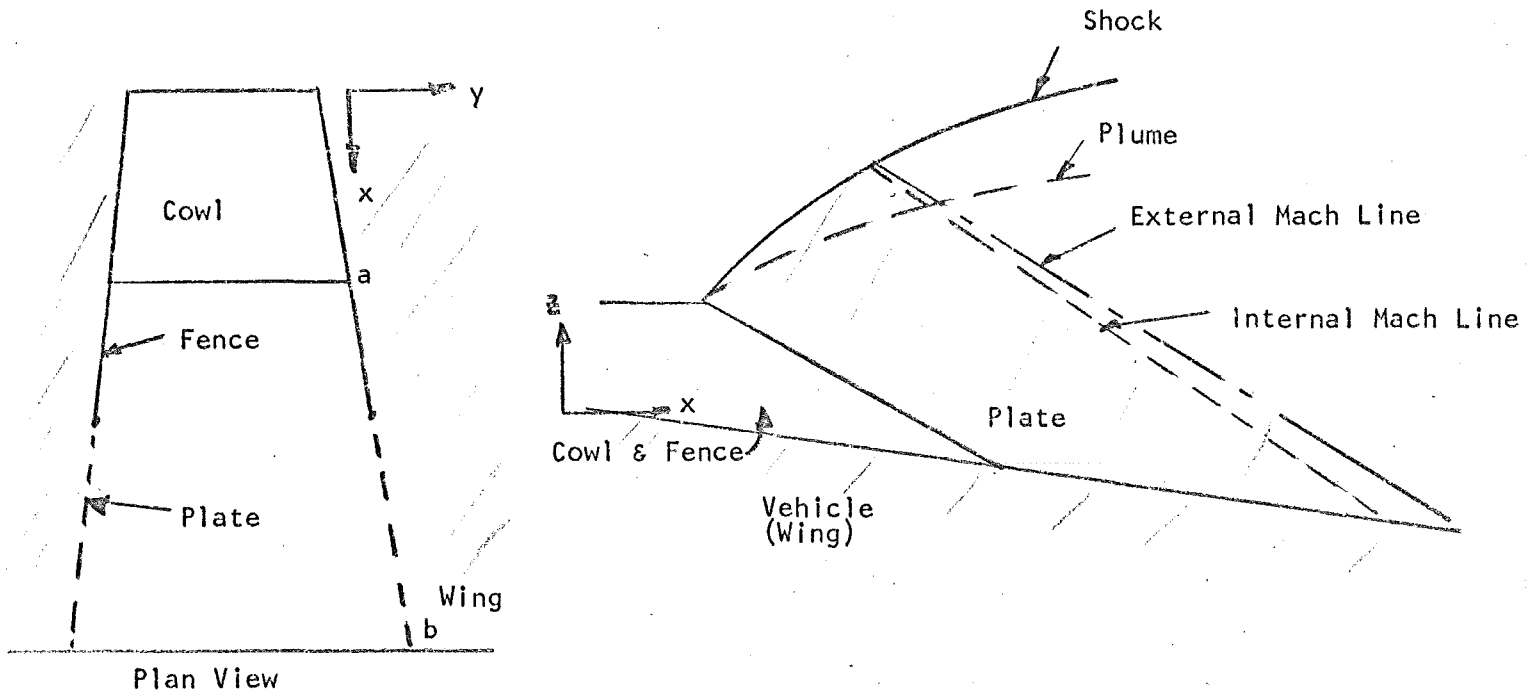
Plan View

FIGURE 13.

Thus the plume interference problem has been reduced to an equivalent quasi two dimensional problem except for the correction introduced above.

    B. Conical Flow Solutions - The cowl can be represented by inter-secting planar surfaces forming corners with included angles of $270°$ (external corner) or $90°$ (internal corner) as in Figure (14). The flow field in each corner is conical, and as will be demonstrated, classical conical flow solutions yield the qualitative nature of the solution, but must be corrected for nonlinear effects introduced by local flow conditions.
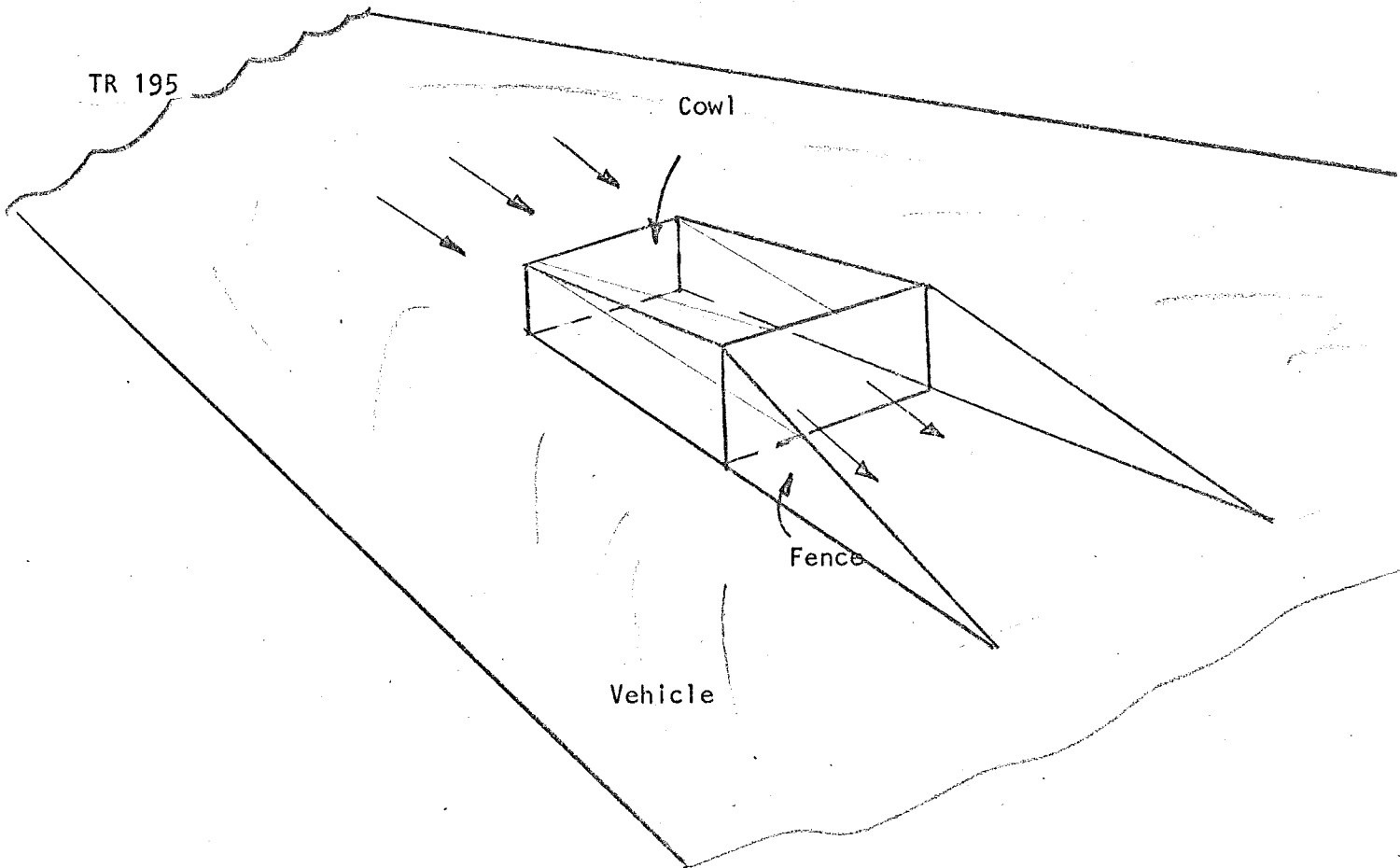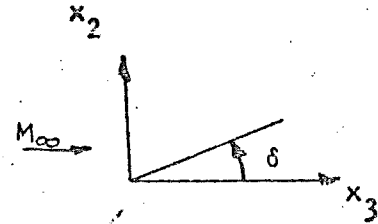
FIGURE 14. COWL AND FENCE

Classical conical flow is one in which the flow properties are constant along rays $t = X_1/X_3$ as in Figure (15). If the X_1 X_3 plane defines a wing of finite span with deflection δ and free stream Mach number $M_\infty > 1$, the flow on the tip region (shaded area, Figure 15) is given by the conical solution,

$$cp = \frac{2\delta}{\pi\beta} \cos^{-1} \left[\left(\frac{\varepsilon - \cos\psi}{1 - \varepsilon \cos\psi} \right) \right]$$

If beyond the wing the boundary condition $\phi_n = o$ (i.e., disturbance velocity) is applied to a plate rotated through an angle $\pi - \nu$ as in Figure (15b), then the solution becomes
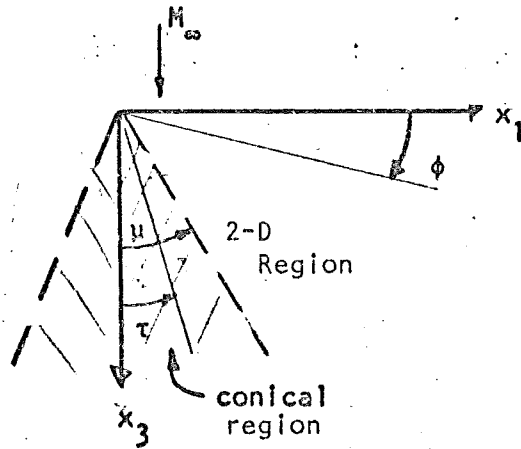
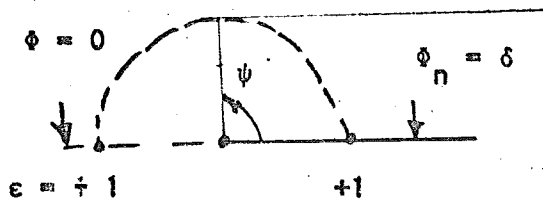$\phi \sim$ Sweep Angle

$t = \tan^{-1} \tau$

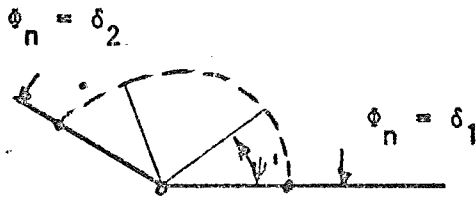$\tau = x_1/x_3$

$\mu = \sin^{-1} \left(\frac{1}{M_\infty}\right)$

$\cos \psi = \tan \phi \, \tan \mu$

$\epsilon = \beta t$

$C_p = \frac{2\delta}{\pi\beta} \cos^{-1} \left[\left(\frac{\epsilon - \cos \psi}{1 - \epsilon \cos \psi}\right) \right]$

$\psi' = \frac{\pi}{\nu} \psi$

$C_p = \frac{2\delta}{\pi\beta} \cos^{-1} \left[-\left(\frac{\epsilon - \cos \psi'}{1 - \epsilon \cos \psi'}\right) \right]$

$C_p = C_{p_{Base}} \left[\pi - \cos^{-1} \left(\frac{\epsilon - \cos \psi'}{1 - \epsilon \cos \psi'}\right) \right.$

$\left. + \delta_2/\delta_1 \cos^{-1} \left(\frac{\epsilon + \cos \psi'}{1 + \epsilon \cos \psi'}\right) \right]$

$C_{p_{Base}} = \frac{2\delta_1}{\beta}$

$\nu = $ dihedral angle

No Dihedral

$\phi = 0$ $\phi_n = \delta$

ψ

$\epsilon = -1$ $+1$

No Dihedral (a)

Plate $\phi_n = 0$

$\pi \div \nu$ ψ' $\phi_n = \delta$ Wing

With Dihedral (b)

$\phi_n = \delta_2$

$\phi_n = \delta_1$

ψ'

Wing with Dihedral (c)

2-D Region

μ

τ

conical region

FIGURE 15

-24-

$$Cp = \frac{2\delta}{\pi\beta} \cos^{-1} \left[-(\frac{\varepsilon - \cos \psi^1}{1 - \varepsilon \cos \psi}1) \right]$$

where $\psi^1 = (\pi/\nu)\psi$

This is a so called dihedral solution, the details of which can be found in References (9),(10) and (11). If the boundary condition $\Phi_n = 0$ is replaced by $\Phi_n = \delta_2$ then by superposition of linear solutions

$$Cp = C_{p\ Base} \left[\pi - \cos^{-1} \left[(\frac{\varepsilon - \cos \psi^1}{1 - \varepsilon \cos \psi^1}1) \right] + \right.$$

$$\left. (\delta_2/\delta_{Base}) \cos^{-1} \left[(\frac{\varepsilon + \cos \psi^1}{1 + \varepsilon \cos \psi^1}1) \right] \right]$$

This represents the solution for a wing with dihedral angle ν. Figure (16) is a plot of the above equation for $\nu = 270^\circ$ (external corner). These results are valid for the parameter $M_\infty \delta < < 1$, i.e., linearized supersonic flow. For $M_\infty \delta \sim 0(1)$ the results can be improved if (δ_2/δ_{base}) is replaced by the ratio of the local 2-D pressure coefficients. For the hypersonic approximation tangent wedge solutions are appropriate for these values.
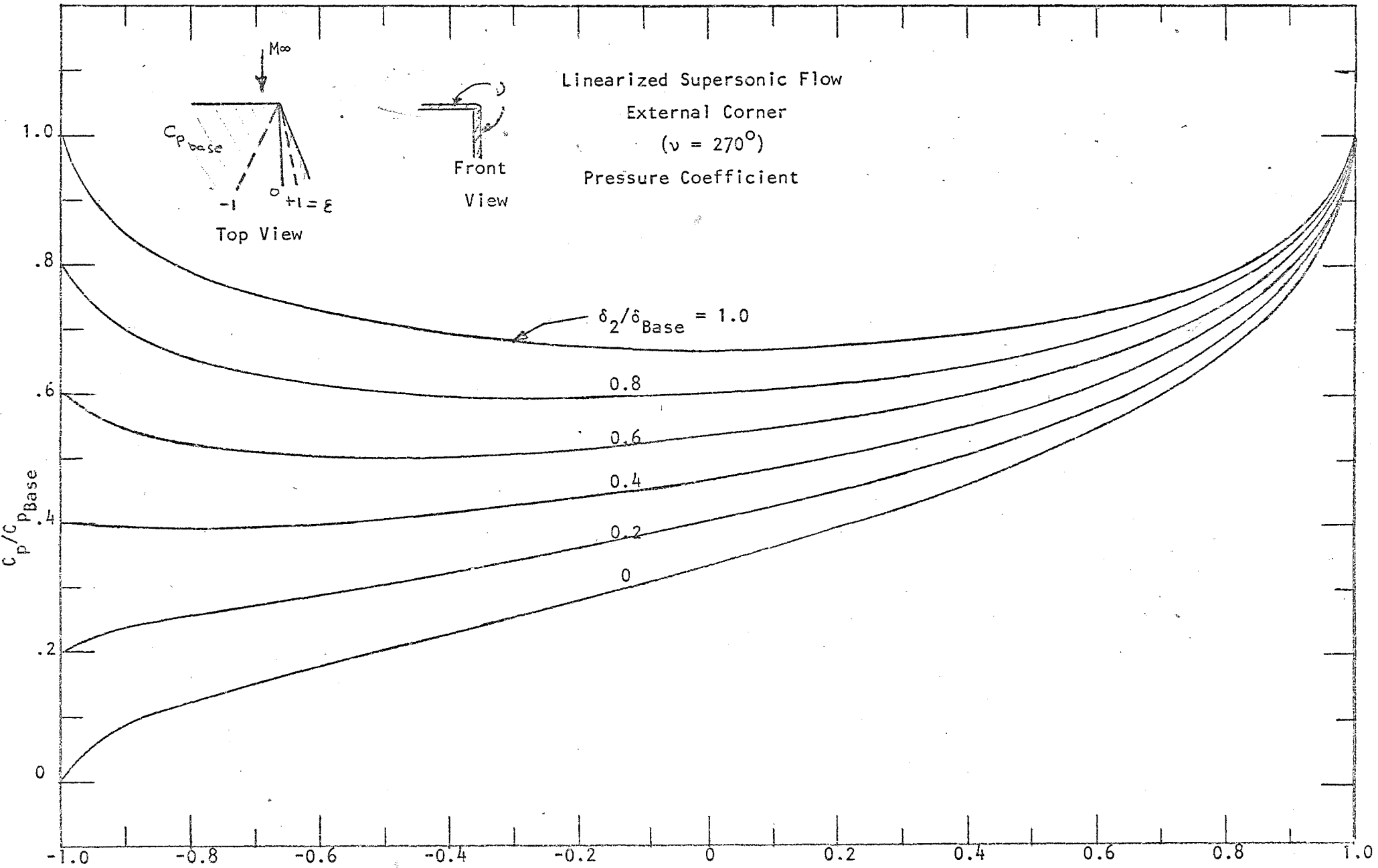
Linearized Supersonic Flow
External Corner
$(\nu = 270^{\circ})$
Pressure Coefficient

$\varepsilon = \beta t$

FIGURE 16

26-

For the internal corner $\left(\nu = 90^{\circ}\right)$ the linearized result reduces to

$$\frac{P-P_{base}}{P_{base}-P_{\infty}} = (\delta_2/\delta_{base})$$

However, Reference (12) indicates that this result considerably under-estimates the interference pressure. For equal wedge angles, $\delta_2 = \delta_{base}$, if the linearized interference pressure is viewed as a perturbation from the base pressure P_{base} then

$$\frac{P-P_{Base}}{P_{Base}} = 1$$

Which agrees with the result of Reference (12) for $M_{\infty} = 3.17$ and $\delta = 12.1^{\circ}$. From the data of References (12) and (13) an approximate correlation of the interference pressure for an internal compression corner has been determined, i.e.:

$$\frac{P-P_b}{P_b} = .026 \left(\frac{\delta}{\delta_b}\right)^2 \sqrt{M_{\infty}^2 - 1} \, \delta_b$$

For $M_{\infty} \delta_b \gg 1$ using the local Mach number rather than M_{∞} correlates the results well even up to $M_{\infty} = 20$.

Given the above local corner solutions the cowl forces can be computed by integrating over the appropriate cowl areas defined by the plane of symmetry and the local Mach cones in the corner.

SECTION V
CONCLUSIONS

The current ATL parametric approach to scramjet nozzle design allows the propulsion specialist to rapidly and logically assess the effects of various parameters on engine and vehicle performance. The three step method of increasing complexity permits one to examine only the most promising configurations selected from the previous step. Thus extraneous and time consuming calculations are eliminated. As part of the above parametric approach ATL has developed, in References (1-5), and has delivered to NASA computer programs based on the level of sophistication required in each step of the optimization process.

The concept of preservation of lift and the use of equivalent two dimensional solutions allows for rapid assessment of the external plume interference problem. In addition, the conical flow solutions developed, significantly simplify the force computation associated with external cowl and fence surfaces.

The integrated parametric methodology described herein is a logical process leading to the optimum vehicle-propulsion system based on the physical constraints imposed by the designer.

CURRENT PROGRAM CAPABILITIES

WAVE PROGRAM		SOURCE FLOW CHARACTERISTICS		THREE DIMENSIONAL PROGRAM	
Advantages	Disadvantages	Advantages	Disadvantages	Advantages	Disadvantages
(1) Ease of use	(1) Limited to uniform initial profile	(1) Arbitrary initial data M>1	(1) More difficult to use	(1) Arbitrary 3-D initial profile	(1) Complex to use
(2) Rapid Calculations	(2) Isentropic, homentropic, constant Φ	(2) Nonisentropic Nonhomentropic Variable Φ	(2) Complex Logic	(2) Computes entire 3-D exhaust nozzle flow field	(2) Complex Logic
(3) Mechanized	(3) Limited to certain wave configurations	(3) Can compute overexpanded & underexpanded (off design) case	(3) Longer running time	(3) H_2-Air equilibrium chemistry	(3) Long running time
(4) Small storage	(4) No external flow interaction	(4) Equilibrium H_2-Air chemistry	(4) Not mechanized (one case at a time)	(4) Three coordinate systems	(4) Not mechanized
(5) Equilibrium H_2-Air or ideal gas	(5) Quasi 2-D	(5) Frozen H_2-Air chemistry	(5) More storage	(all 3D) cart x,y,z cyl. x,θ, r line source r,θ, z	(5) Maximum core storage
		(6) Three coordinate systems 2-D Cartesian x,y Cylindrical x,r Source flow r,y	(6) quasi 2D		(6) Isentropic

REFERENCES

(1) Dash, S., Del Guidice, P., and Kalben, P., "A Numerical Procedure for the Parametric Optimization of Three Dimensional Scramjet Nozzles," ATL TR 188, Oct. 1973.

(2) Del Guidice, P., Dash, S., and Kalben, P., "A Source Flow Characteristic Technique for the Analysis of Scramjet Exhaust Flow Fields," ATL TR 186, March 1974.

(3) Kalben, P., "A Manual for a Source Flow Characteristics Program," ATL TM-179, April 1974.

(4) Dash, S. and Del Guidice, P., "Analysis and Design of Three Dimensional Supersonic Nozzles" - Vol. 1, "Nozzle-Exhaust Flow Field Analysis by a Reference Plane Characteristic Technique," NASA CR 13250, Oct. 1972.

(5) Kalben, P., Vol. II of Above, "Numerical Program for Analysis of Nozzle-Exhaust Flow Fields,: NASA CR 13235, Oct. 1972.

(6) Dash, S. and Del Guidice, P., "Three Dimensional Nozzle Exhaust Flow Field Analysis by a Reference Plane Technique," AIAA Paper No. 72-704, June 1972.

(7) Lagerstrom, P. A., and Van Dyke, M.D., "General Considerations About Planar and Non-Planar Lifting Systems," Douglas Aircraft Co., Report No. SM-13432, June 1949.

(8) Ferri, A., Clarke, J.M. and Ting, L., "Favorable Interference in Lifting Systems in Supersonic Flow," Journal of Aeronautical Sciences, November 1957.

(9) Ting, L., "Diffraction of Disturbances Around a Convex Right Corner with Applications in Acoustics and Wing Body Interference," Journal of Aeronautical Sciences, November 1957.

(10) Snow, R.M., "Aerodynamic Characteristics of Wings at High Speeds," John Hopkins University, Applied Physics Laboratory, March 1947. Bumblebee Report No. 55 (AD 634865).

(11) Ting, L ., "Pressure Distribution on Dihedral Wings at Supersonic Speed," Polytechnic Institute of Brooklyn, Jan. 1958, AFOSR TN 58-86, (AD 148135).

(12) Charwat, A.F. Redekeopp, L.G., "Supersonic Interference Flow Along the Corner of Intersecting Wedges," AIAA Journal Volume 5, March 1967.

(13) Watson, R.D., Weinstein, L.M., "A Study of Hypersonic Corner Flow Interactions," AIAA Journal, Volume 9, July 1971.